PHYSICAL REVIEW A **70**, 031602(R) (2004)

Bose-Einstein condensation at constant temperature

M. Erhard, H. Schmaljohann, J. Kronjäger, K. Bongs, and K. Sengstock
Institut für Laser-Physik, Universität Hamburg, Luruper Chaussee 149, 22761 Hamburg, Germany
(Received 30 January 2004; published 8 September 2004)

We present an experimental approach to Bose-Einstein condensation by increasing the particle number of the system at almost constant temperature. In particular, the emergence of a new condensate is observed in multicomponent $F=1$ spinor condensates of ^{87}Rb. Furthermore, we develop a simple rate-equation model for multicomponent Bose-Einstein condensate thermodynamics at finite temperature which well reproduces the measured effects.

DOI: 10.1103/PhysRevA.70.031602 PACS number(s): 03.75.Nt, 03.75.Hh, 03.75.Mn

The experimental realization of Bose-Einstein condensates (BECs) in dilute atomic gases [1–3] and the breathtaking emergence of fascinating physics of cold quantum gases in an increasing number of experiments have had formative influence on the common model usually used for the description of Bose-Einstein condensation (see, e.g., [4], and references therein). This model is based on a system of constant particle numbers whose temperature T is reduced. The popularity of this approach arises from the fact that all experiments so far make use of evaporative cooling techniques which reduce the temperature of the sample (at the expense of particle losses). This path to-quantum degeneracy is illustrated in the phase diagram of Fig. 1. Starting with a certain particle number N, the temperature T of the system is reduced below the critical temperature $T_c(N)$, which leads to an accumulation of particles in the condensate fraction N_0/N. Detailed experimental studies [5–7] have compared this quantity with theoretical descriptions.

In this paper we present a completely different experimental realization of Bose-Einstein condensation by increasing the particle number of a system at almost constant temperature. The corresponding path is also marked in Fig. 1 and leads to BECs almost orthogonally to the common route discussed above. We start with $N=0$ and add more and more particles at nearly constant temperature T until the critical particle number $N_c(T)$ is reached, i.e., the population of the thermal cloud saturates and all further added particles fill up the condensate fraction. It is worth mentioning that this approach corresponds to the original idea used by Einstein [8] and theoretical descriptions over decades to discuss BECs. Furthermore, first attempts to achieve quantum degeneracy in spin-polarized hydrogen [9,10] were based on increasing density by adding particles and by compression at liquid helium temperatures. Another approach demonstrated Bose-Einstein condensation by changing the trapping potential geometry [11,12].

The thermodynamical approach to BECs discussed in this paper is realized in multicomponent BECs, which provide multiple internal quantum states of the involved atoms. We want to emphasize that these systems open up a rich variety of thermodynamical aspects as the involved finite temperature dynamics is extended to more components which are additionally coupled and influence each other. The thermodynamical description has to take into account all interactions between multiple condensate components and just as many thermal clouds (we use this term instead of "normal components"). In this context recent experiments have observed "decoherence-driven cooling" [13] and melting of new condensate components [14].

The system considered here is based on a $F=1$ spinor condensate of ^{87}Rb with three internal states $m_F=-1,0,+1$. The main idea is to increase the particle number in the initially unpopulated $m_F=0$ spin component via spin dynamics transfer out of the other components. For this we first prepare a partially condensed mixture of the $|-1\rangle$ and $|+1\rangle$ states. The resulting dynamics can be divided into two main successive steps which are illustrated in Fig. 2 as (a) and (b).

The first process is that spin dynamics populates the $m_F=0$ state by converting $m_F=\pm 1$ condensate atoms into $m_F=0$ atoms according to $|+1\rangle+|-1\rangle \leftrightarrow |0\rangle+|0\rangle$ [14–17]. Due to its density dependence, spin dynamics is practically restricted to the condensed fractions, resulting in the production of $m_F=0$ "condensate" atoms, which, however, immediately thermalize into the $m_F=0$ thermal cloud due to collisions with all thermal clouds [Fig. 2(a)]. We want to emphasize at this point that thermalization is the fastest timescale ($\approx$50 ms) of our system and therefore spin dynamics ($\approx$1 s) is only a means to produce the new component. The redistribution of constant total energy among more thermal atoms during this process leads as a side effect to a

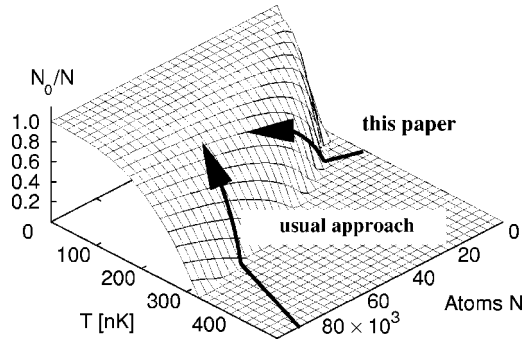

FIG. 1. Phase diagram of Bose-Einstein condensation for a typical ^{87}Rb experiment. The condensate fraction (if >0) is plotted as $N_0/N=1-g_3(1)[k_B/(\hbar\bar{\omega})]^3T^3/N$. The usual realization of BECs is done by decreasing T at (almost) constant particle number N. In this paper condensation by increasing particle number starting with $N=0$ at (nearly) constant temperature is discussed.

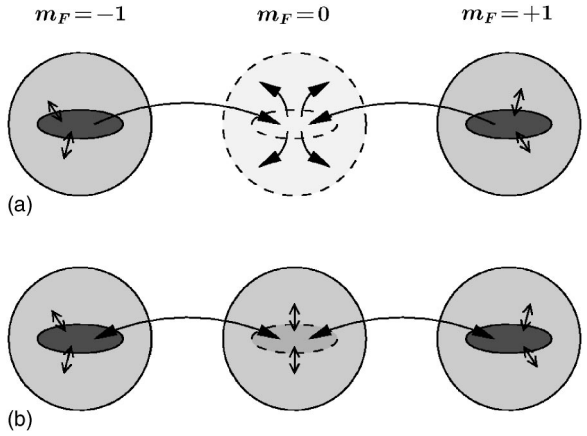

FIG. 2. Scheme of the dynamics. (a) Spin dynamics transfers population to the $m_F=0$ state, which thermalizes almost immediately. (b) When all thermal clouds are equally populated and thus the critical particle number in $m_F=0$ is reached, a condensate arises and "free" spin dynamics can take place.

decrease of temperature T. This is similar to "decoherence-driven cooling" of another experiment [13] which in contrast to our system did not involve conversion between different condensate components.

As soon as the critical particle number in the $m_F=0$ thermal cloud is reached, the phase transition in the $m_F=0$ component takes place and a condensate fraction emerges [Fig. 2(b)]. From this moment on the thermal clouds are and remain equally populated and provide a constant temperature reservoir of the system. Therefore, "free" spin dynamics may take place between the spin components of the condensate fractions, i.e., at a constant total number of condensed atoms but still in touch with the reservoir of finite temperature. Thus spin dynamics mainly determines the final m_F condensate fractions, which are not as a rule equally populated in contrast to the thermal clouds [18].

The experimental setup (for details see [14,19]) produces BECs in an optical dipole trap which provides a spin-independent trapping potential. The trapping frequencies are $2\pi\times 890$ Hz vertically, $2\pi\times 160$ Hz horizontally, and $2\pi\times 20$ Hz along the beam direction. Spin dynamics is suppressed during preparation of the initial spin state due to the high magnetic offset field of 25 G, which is subsequently lowered to a value of 340 ± 20 mG to allow for spin dynamics. After a variable hold time of $0-30$ s the dipole trap is switched off and the released atoms are spatially separated by a Stern-Gerlach gradient. Finally, an absorption image is taken in order to determine BEC and thermal atom numbers by a simultaneous fit of three parabolas and three Gaussians for the three m_F components.

Figure 3 shows the experimentally obtained BEC and thermal atom numbers versus the hold time compared to simulations of the rate-equation model, which will be presented later. We start with an initial mixture of $m_F=\pm 1$ both in BECs and thermal fractions. The preparation process leads to a remaining population of $<10\%$ in the $m_F=0$ state.

The experimental data demonstrate all of the previously introduced dynamics only modified by loss processes. First a $m_F=0$ thermal cloud arises and grows until the critical particle number is reached after $5-10$ s. Note, this is the moment of equal populations of all thermal clouds. Subsequently, a $m_F=0$ condensate fraction emerges. The data between 5 and 10 s suggest that the exact moment of phase transition varies from shot to shot. Indeed, this moment crucially depends on spin dynamics as will be discussed later. Finally, spin dynamics leads to a steady state which decreases due to loss processes with an experimentally observed relative condensate distribution of $40-45\%$ $m_F=\pm 1$ and $10-20\%$ $m_F=0$ [20].

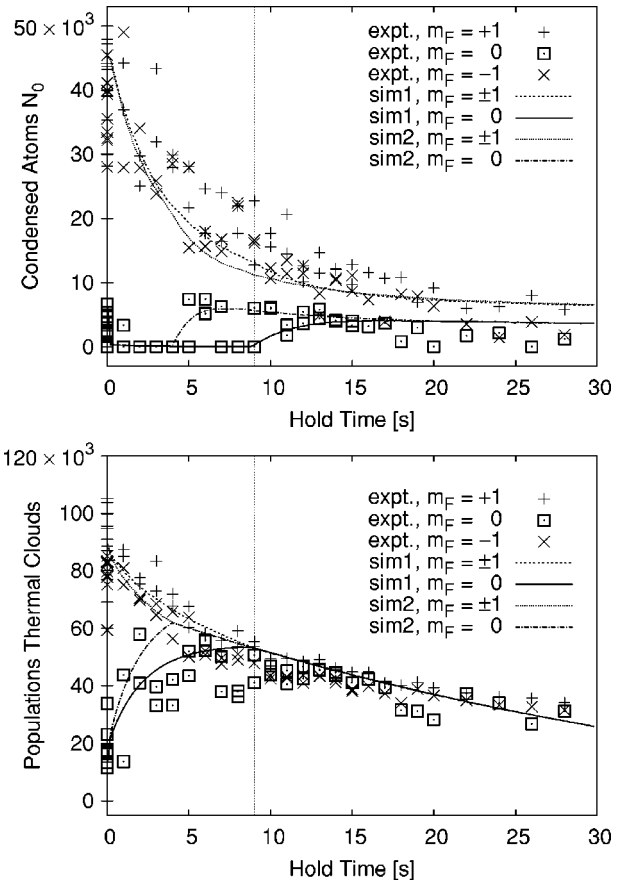

FIG. 3. Measured condensate and thermal atom numbers for the different spin states (marked as "expt.") as functions of different hold times. The lines represent solutions of the rate-equation model for two different sets of spin dynamics parameters denoted as "sim1" and "sim2" (see text for numbers). The moments when the critical particle number for $m_F=0$ is reached in the simulations are marked by vertical lines.

In the following we develop a simple rate-equation model, which reproduces the main experimental observations. We do not intend to give a detailed and thorough simulation of a finite temperature BEC, which would be quite involved and is the subject of current theoretical activities [21–24]. Rather, a basic model from a experimentalist's point of view is presented to stimulate a vivid discussion of finite temperature effects in multicomponent BECs and introduce a number of single processes which yield the observed behavior. The model is based on a set of 7 variables N_0^-, N_0^0, N_0^+, N_t^-, N_t^0, N_t^+, T, where N_0^X with $X=-,0,+$ denote the atom numbers of $m_F=-1,0,+1$ in the condensate fraction and N_t^X

the respective atom numbers in the thermal cloud. T is the system temperature and assumed to be equal for all components. The equations of motion read

$$\dot{N}_0^X = \dot{N}_{0,th}^X + \dot{N}_{0,sp}^X + \dot{N}_{0,1b}^X + \dot{N}_{0,3b}^X,$$

$$\dot{N}_t^X = \dot{N}_{t,th}^X + \dot{N}_{t,1b}^X + \dot{N}_{t,ev}^X,$$

$$\dot{T} = \dot{T}_{th} + \dot{T}_{ev},$$

and include the processes thermalization $(\dot{N}_{\star,th}^X, \dot{T}_{th})$, spin dynamics $(\dot{N}_{0,sp}^X)$, one-body losses $(\dot{N}_{\star,1b}^X)$, three-body losses $(\dot{N}_{0,3b}^X)$, and evaporation $(\dot{N}_{t,ev}^X, \dot{T}_{ev})$. These single effects as well as an additionally introduced phase-space redistribution will be discussed in the following.

The thermalization rate γ_{th} quantifies the collisional transfer of condensed atoms into the thermal component

$$\dot{N}_{0,th}^X = -\tilde{\gamma}_{th} N_0^X N_t,$$

$$\dot{N}_{t,th}^X = +\tilde{\gamma}_{th} N_0^X N_t,$$

where $N_t = N_t^- + N_t^0 + N_t^+$ and $\tilde{\gamma}_{th}$ is obtained via the relation $\tilde{\gamma}_{th} N_t = \gamma_{th} \hat{n}_t$ which takes into account the peak density of the thermal cloud $\hat{n}_t$ to convert the density-dependent rate γ_{th} into $\tilde{\gamma}_{th} = \gamma_{th} \bar{\omega}^3 [m/(2\pi k_B T)]^{(3/2)}$. The temperature and spin dependence of γ_{th} is neglected. The system temperature T decreases as the conserved total energy is redistributed among more thermal atoms

$$\dot{T}_{th} = -T \tilde{\gamma}_{th} N_0,$$

with $N_0 = N_0^- + N_0^0 + N_0^+$. The used value $\gamma_{th} = 10^{-18}$ m^3/s leads to a thermalization rate $\tilde{\gamma}_{th} N_0$ of ≈ 13 1/s for $N_0 = 45\,000$, which corresponds to our experiment.

Spin dynamics is implemented by a simple coupling of the condensate atoms due to the relation $|-1\rangle + |+1\rangle \leftrightarrow |0\rangle + |0\rangle$ with two reaction rates $\tilde{\gamma}_{sp1}$ and $\tilde{\gamma}_{sp2}$ for forward and backward reactions [25]

$$\dot{N}_{0,sp}^{\pm} = \tilde{\gamma}_{sp1} N_0^0 N_0^0 - \tilde{\gamma}_{sp2} N_0^- N_0^+,$$

$$\dot{N}_{0,sp}^0 = -2\tilde{\gamma}_{sp1} N_0^0 N_0^0 + 2\tilde{\gamma}_{sp2} N_0^- N_0^+.$$

One-body loss occurs independently of the spin state and equally in the BEC and thermal cloud. The rate used is $\gamma_1 = 0.011$ 1/s and corresponds to the measured $1/e$ lifetime of 90 s limited by background gas collisions

$$\dot{N}_{0,1b}^X = -\gamma_1 N_0^X,$$

$$\dot{N}_{t,1b}^X = -\gamma_1 N_t^X.$$

For three-body loss [26] we assume a spin-independent process, ignore possible changes in statistical factors due to multiple components and obtain

$$\frac{\dot{N}_{0,3b}^X}{N_0^X} = -Lc_3 (N_0)^{4/5},$$

with $c_3 = 7/6c_2^2$ and $c_2 = 15^{2/5}(14\pi)^{-1}(m\bar{\omega}/\hbar\sqrt{a})^{6/5}$. The loss rate used is $L = 5.8 \times 10^{-42}$ m^6/s [27].

The evaporation process due to finite trap depth $k_B T_e$ is implemented by a particle loss of the thermal cloud connected with a decrease of the system temperature. The temperature dependence of the evaporation rate γ_e is neglected and the loss reads

$$\dot{N}_{t,ev}^X = -\gamma_e N_t^X.$$

Energy conservation leads to a change of temperature

$$\dot{T}_{ev} = \gamma_e (T - T_e).$$

We use the Euler method to propagate the equations in discrete time steps of duration Δt [e.g., $N_0^X(t+\Delta t) = N_0^X(t) + \dot{N}_0^X \Delta t$]. After each simulation step a phase-space redistribution is carried out. This is important to introduce quantum statistics into the equations. If the critical density in the thermal cloud is exceeded, population is transferred into the condensate fraction to fulfill statistics. Therefore, the critical particle number is calculated as $N_c = g_3(1)[k_B T/(\hbar\bar{\omega})]^3$ [28] and the following condition is checked for $X = -, 0, +$.

$$\text{If } (N_t^X > N_c): N_0^X(t+\Delta t) = N_0^X(t) + (N_t^X(t) - N_c)$$

$$N_t^X(t+\Delta t) = N_c.$$

This recondensation step is related to a temperature change obtained by total energy conservation as

$$T(t+\Delta t) = T(t)\left[1 + \frac{N_0(t+\Delta t) - N_0(t)}{N_t(t+\Delta t)}\right].$$

The thermalization step and the phase-space redistribution cancel out in the case of thermal equilibrium resulting in steady condensate fractions and constant temperature. Nevertheless, these steps are crucial to describe the occurrence of the thermal components and condensate fractions. As thermalization is the fastest time scale of the considered system, a steplike description seems to be reasonable.

Our rate-equation model reproduces all experimentally observed thermal features even with a reasonable quantitative accuracy as shown in Fig. 3. The initial condensate populations were chosen as $N_0^-(0) = N_0^+(0) = 45000$, $N_0^0(0) = 7000$ and the thermal atom numbers as $N_t^-(0) = N_t^+(0) = 90\,000$ and $N_t^0(0) = 12\,000$ and $T(0) = 288$ nK. Evaporation parameters are $\gamma_e = 0.015$ 1/s and $T_e = 500$ nK. Simulations for two sets of spin dynamics rates [29] $\tilde{\gamma}_{sp1} = 1.6 \times 10^{-5}$ 1/s, $\tilde{\gamma}_{sp2} = 0.4 \times 10^{-5}$ 1/s (sim1), and $\tilde{\gamma}_{sp1} = 2.4 \times 10^{-5}$ 1/s, $\tilde{\gamma}_{sp2} = 0.6 \times 10^{-5}$ 1/s (sim2) have been carried out. Although these two sets differ by only 33%, the resulting moment of condensation varies by more than a factor of 2 (4 and 9 s, respectively). Indeed we have to assume that there is a shot-to-shot variation of spin dynamics in our experiment as initial phases are not controlled. It has been theoretically shown [30] that spin dynamics crucially depends on initial relative phases. Another influence on the spin dynamics rates

may arise from shot-to-shot varying densities.

In its simplicity the rate-equation model allows us to obtain a clear physical picture of the dominant thermodynamical aspects but it lacks coherent spin dynamics, which has been reduced to simple rate equations. This procedure seems to be suitable for the discussed regime and may be applied to further problems in this context. Nevertheless the detailed treatment of shot-to-shot variations, coherent dynamics, excitations, and phase fluctuations of condensates [31] requires an extended theoretical description.

Finally, we want to point out that the complementary case has been studied for $F=2$ of ^{87}Rb [14], where spin dynamics ($\approx$10 ms) is faster than thermalization ($\approx$50 ms) leading first to a steady distribution of condensate spin components which afterwards melt.

In conclusion, we have reported the experimental realization of a regime of Bose-Einstein condensation in spinor condensates. The physics introduced here paves the way towards general aspects in multicomponent quantum gas thermodynamics at finite temperature as particle numbers and temperature of the system and reservoir can be adjusted in a variety of configurations. In this context, thermodynamically driven spin alignment of a condensate has been observed [32].

We acknowledge support from the DFG-SPP 1116.

[1] M. H. Anderson *et al.*, Science **269**, 198 (1995).
[2] K. B. Davis *et al.*, Phys. Rev. Lett. **75**, 3969 (1995).
[3] C. C. Bradley, C. A. Sackett, J. J. Tollett, and R. G. Hulet, Phys. Rev. Lett. **75**, 1687 (1995); *ibid.* **79**, 1170 (1997).
[4] L. P. Pitaevskii and S. Stringari, *Bose-Einstein Condensation* (Oxford University Press, Oxford, 2003).
[5] J. R. Ensher *et al.*, Phys. Rev. Lett. **77**, 4984 (1996).
[6] M.-O. Mewes *et al.*, Phys. Rev. Lett. **77**, 416 (1996).
[7] F. Gerbier *et al.*, Phys. Rev. Lett. **92**, 030405 (2004).
[8] A. Einstein, Sitzungsber. Preuss. Akad. Wiss., Phys. Math. Kl. **1925**, 3 (1925).
[9] J. T. M. Walraven and I. F. Silvera, Phys. Rev. Lett. **44**, 168 (1980).
[10] R. A. Cline, D. A. Smith, T. J. Greytak, and D. Kleppner, Phys. Rev. Lett. **45**, 2117 (1980).
[11] D. M. Stamper-Kurn *et al.*, Phys. Rev. Lett. **81**, 2194 (1998).
[12] P. W. H. Pinkse *et al.*, Phys. Rev. Lett. **78**, 990 (1997).
[13] H. Lewandowski, J. McGuirk, D. Harber, and E. Cornell, Phys. Rev. Lett. **91**, 240404 (2003).
[14] H. Schmaljohann *et al.*, Phys. Rev. Lett. **92**, 040402 (2004).
[15] T.-L. Ho, Phys. Rev. Lett. **81**, 742 (1998).
[16] T. Ohmi and K. Machida, J. Phys. Soc. Jpn. **67**, 1822 (1998).
[17] J. Stenger *et al.*, Nature (London) **396**, 345 (1999).
[18] Details of spin dynamics (see, e.g., [14–17]) are not important here and go beyond the scope of this paper.
[19] M. Erhard *et al.*, Phys. Rev. A **69**, 032705 (2004).
[20] We note that the zero temperature ground state of the $F=1$ spinor system [15–17,33] is not reached here (for our parameters the calculated ground state consists of 10% $m_F=\pm1$ and 80% $m_F=0$). In contrast to recent investigations which verified the predicted $F=1$ energetic ground state [14,34] we start with $T>0$ and unfavorable initial populations with respect to the ground state. Damping of spin dynamics due to finite temperature and magnetic field may explain this discrepancy.
[21] C. W. Gardiner and P. Zoller, Phys. Rev. A **61**, 033601 (2000).
[22] K. Góral, M. Gajda, and K. Rzążewski, Phys. Rev. A **66**, 051602 (2002).
[23] B. Jackson and E. Zaremba, Phys. Rev. A **66**, 033606 (2002).
[24] S. A. Morgan, M. Rusch, D. A. W. Hutchinson, and K. Burnett, Phys. Rev. Lett. **91**, 250403 (2003).
[25] Numerical simulations of a set of coupled Gross-Pitaevskii equations turned out to be cumbersome as they crucially depend on initial phases [30]. The considerable effect of spin dynamics here is the production of $|0\rangle$ atoms. The introduction of two rates following the law of mass action is a simple approximation for spin dynamics reaching a (nonequally distributed) steady state.
[26] J. Söding *et al.*, Appl. Phys. B: Lasers Opt. **69**, 257 (1999).
[27] E. A. Burt *et al.*, Phys. Rev. Lett. **79**, 337 (1997).
[28] We neglect small shifts due to interactions and trapping.
[29] The spin-dependent energy $g_2\overline{n}/2\langle\vec{F}\rangle^2$ [15–17,33,34] suggests a rate $\gamma_{sp}=g_2\overline{n}/(2\hbar)=-20.7\ 1/\mathrm{s}$ for our parameters. Assuming $\gamma_{sp}=\dot{N}_0^0/N_0^0$, this compares to $\tilde{\gamma}_{sp2}\approx\gamma_{sp}N_0^0(0)/[2N_0^-(0)N_0^+(0)]=3.6\times10^{-5}\ 1/\mathrm{s}$ for the initial time.
[30] C. Law, H. Pu, and N. Bigelow, Phys. Rev. Lett. **81**, 5257 (1998).
[31] D. S. Petrov, G. V. Shlyapnikov, and J. T. M. Walraven, Phys. Rev. Lett. **87**, 050404 (2001).
[32] M. Erhard *et al.* (unpublished).
[33] W. Zhang, S. Yi, and L. You, New J. Phys. **5**, 77.1 (2003).
[34] M.-S. Chang *et al.*, Phys. Rev. Lett. **92**, 140403 (2004).